Optically induced dynamics of muonium centers in Si studied via their precession signatures

I. Fan,[1,*] K. H. Chow,[1,†] B. Hitti,[2] R. Scheuermann,[3] W. A. MacFarlane,[4] A. I. Mansour,[1] B. E. Schultz,[1] M. Egilmez,[1] J. Jung,[1] and R. L. Lichti[5]

[1]*Department of Physics, University of Alberta, Edmonton, Alberta, Canada T6G 2G7*

[2]*TRIUMF, 4004 Wesbrook Mall, Vancouver, British Columbia, Canada V6T 2A3*

[3]*Paul Scherrer Institute, CH-5232 Villigen, PSI Switzerland*

[4]*Department of Chemistry, University of British Columbia, Vancouver, British Columbia, Canada V6T 1Z1*

[5]*Department of Physics, Texas Tech University, Lubbock, Texas 79409-1051, USA*

(Received 20 September 2007; published 7 January 2008)

We studied the influence of the optical excitation on three muonium centers Mu_T^0, Mu_{BC}^0, and Mu_{BC}^+ in high resistivity silicon. These investigations were carried out on the spin precession signature of each center as a function of temperature. It is found that photoexcitation resulted in significant enhancements of the depolarization rates of the precession signals as the three muonium centers underwent interactions with photogenerated free carriers. The results are described by a three-state model involving transitions between Mu_T^0, Mu_{BC}^0, and Mu_{BC}^+ as well as spin exchange processes.

DOI: 10.1103/PhysRevB.77.035203 PACS number(s): 76.75.+i, 72.20.Jv, 71.20.Mq

I. INTRODUCTION

Hydrogen (H) is a technologically important impurity that dramatically modifies the electrical and optical properties of Si and many other semiconductors.[1,2] This often occurs because hydrogen quickly passivates many types of defects in these materials, leading to both detrimental (e.g., passivation of shallow intentional dopants) and beneficial (e.g., passivation of dangling bonds) consequences. In certain semiconductors, H can even act as a shallow dopant.[3] A complete understanding of the behavior of H in semiconductors requires a comprehensive knowledge of the role of *isolated* hydrogen, i.e., the precursor state in many situations, in the semiconductor. However, the rapid reactivity of hydrogen means that many of the techniques that are used to investigate hydrogen in semiconductors are not able to probe isolated H. Studies of muonium ($Mu^0=\mu^+e^-$) using the muon spin rotation/relaxation/resonance (μSR) techniques are now widely recognized to be the main experimental source of information on isolated H in many semiconductors.[4–23]

Recall that the muon (μ^+) is a radioactive particle with a lifetime of ≈ 2.2 μs. It can be considered a pseudoisotope of hydrogen with $\approx \frac{1}{9}$th the mass of the proton, but is still much heavier than the electron ($\approx 200\times$). Hence, the electronic structures of Mu^0 and H^0 are very similar. However, the significantly different masses imply that certain processes, such as those involving diffusion, can be dramatically different. When μ^+ is implanted into high resistivity silicon, three muonium centers are formed. At low temperatures, two neutral muonium states have been experimentally identified, commonly labeled in the literature as Mu_T^0 and Mu_{BC}^0. The Mu_T^0 center is believed to diffuse rapidly through the lattice via tetrahedral interstitial sites and, consequently, has an isotropic hyperfine interaction (≈ 2000 MHz) that is approximately half that of muonium in vacuum.[4] The Mu_{BC}^0 state is located at the Si-Si bond center (BC) and therefore has an anisotropic hyperfine interaction.[24] This interaction is axially symmetric about a $\langle 111\rangle$ crystalline axis and is described by two parameters $A_\parallel$ and $A_\perp$, which are approximately an order of magnitude smaller than the Fermi contact interaction[25] of Mu_T^0, i.e., $A_\parallel=-16.82$ MHz and $A_\perp=-92.59$ MHz. At elevated temperatures, these neutral centers convert into the positively charged muonium center, Mu_{BC}^+.[4] If a significant concentration of free electrons is present in the sample, such as in *n*-type Si, additional dynamical processes involving the various muonium centers are observed. In one such process, often called *spin exchange*, the electron spin on Mu^0 "flips" due to scattering with a free carrier.[11,26] Another process is *cyclic charge exchange* (or *charge-state fluctuation*)[27] whereby the charge state of a muonium center fluctuates between two states: For example, at sufficiently high temperatures, Mu^0 ionizes but captures a free electron within its lifetime, and hence enters a cyclic charge changing process. Furthermore, if the electron concentration exceeds $\approx 10^{14}$ cm^{-3}, a fourth muonium state Mu_T^- can be formed.[28]

Instead of doping the Si with impurities, another method of introducing free charge carriers is by using optical excitation to *athermally* generate electron-hole pairs. Provided that muonium has time to undergo significant interactions with these carriers prior to its decay, photoexcitation experiments enable additional carrier capture processes, which would otherwise not take place in an unilluminated sample at a given temperature. Hence, this is a potentially powerful way to probe muonium dynamical processes involving interactions with free carriers.

Previous studies of muonium in Si (and other semiconductors) using photoexcitation have primarily been carried out[29,30] at pulsed muon facilities using the conventional longitudinal field (LF)-μSR technique.[5] By investigating the amplitude and $1/T_1$ relaxation rates of the muon polarization, dynamics involving the three muonium states and the free carriers are implicitly observed. These dynamics include charge-state changes and site changes. The interpretation of such longitudinal field data is often complicated by the fact that the polarization consists of contributions from all the muonium states that are simultaneously present in the sample at that particular temperature, making it difficult to separate out the effects of optical excitation on a particular center.

Moreover, the dynamics and the muonium center(s) involved in the interactions at a particular temperature can only be revealed by studying the amplitude and relaxation rates at many fields. This implies that conducting a detailed temperature-dependent study of the influence of light on the multiple muonium centers is a very time-consuming process and hence impractical given the limited access to μSR facilities. Studies of photoexcited Si combined with radio-frequency (rf) measurements have also been reported.[31] Only the behavior of the diamagnetic state was studied in these measurements. It was found that illumination has pronounced effects on the corresponding rf-μSR signal.

Another way to investigate photoexcited muonium dynamics is by monitoring the effects of light on the *precession signatures* of the muonium centers directly. Recall that since the hyperfine interactions of Mu^0_{BC}, Mu^0_T, and the diamagnetic center are all different, a unique set of precession frequencies is associated with each of the three states. This provides an unambiguous identification of the state that is involved. Furthermore, since coherent precession will only be observed if the particular muonium state is formed "promptly," the initial states can be selected out. Hence, such studies should complement those carried out with the LF-μSR and rf-μSR techniques. These experiments are best carried out at continuous muon facilities because the precession frequencies are often fast and hence not observable at pulsed muon facilities.[5] In addition, at continuous muon facilities, higher relaxation rates can be investigated. The disadvantage, compared to experiments at pulsed muon facilities, is that the light should be intense enough to produce sufficient carriers for interactions with muonium, yet must not be so bright that significant heating of the sample occurs. Studies of the optically induced changes of the precession signals are sparse. An early study of the diamagnetic precession signature under photoexcitation has been carried out at low temperatures (below $\approx$40 K) in doped Si. It was found the diamagnetic relaxation can be enhanced by illumination.[32]

In this paper, we demonstrate that the precession signatures of all the muonium states in silicon can indeed be strongly modified by optical excitation. In particular, the depolarization rates of the precession signals are dramatically enhanced, and their temperature dependence can be modeled by a three-state model involving transitions between Mu^0_T, Mu^0_{BC}, and Mu^+_{BC}, provided that interactions with photogenerated carriers are incorporated.

II. EXPERIMENTAL SETUP

The optical excitation experiments described in this paper were carried out at the M15 and M20 beamlines at the Tri-University Meson Facility (TRIUMF) located in Vancouver, Canada, where μSR, β-NMR,[33] and β-NQR[34] experiments can be carried out. Positive muons with $\approx$100% polarization and nominal momentum 29.8 MeV/c were implanted into the sample. The sample was obtained from Siltronix, and is a single-side polished, float-zone, high resistivity (10–30 kΩ cm), slightly boron doped silicon wafer with thickness of 600 nm and orientation $\langle 100 \rangle$.

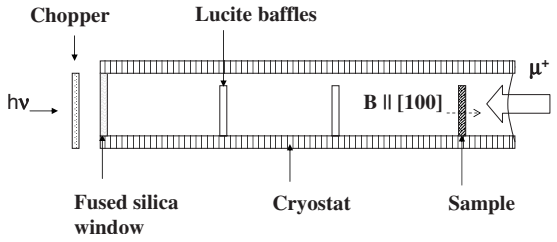

FIG. 1. Schematic diagram of the μSR cryostat for the optical excitation experiment. The incoming μ^+ can be polarized to be either transverse or longitudinal to the applied magnetic field direction.

The schematic of the optical cryostat is summarized in Fig. 1. The sample was mounted on a thin lucite plate inside a horizontal helium gas flow cryostat with a transparent silica window on its backside. (Additional lucite baffles were present to disrupt the flow of helium and provide reasonable cooling efficiency.) A broad spectrum lamp (Gilway Technical L7390) was used to illuminate the (unpolished) side of the sample through the window, while the muons were implanted into the front (polished) side of the sample. The interior wall of the cryostat was covered with a highly reflective Mylar sheet to increase the amount of light that traveled down the length of the cryostat. The light beam was modulated on/off by placing a Boston Electronics SH-20-L-5 optical shutter in the path of the light (which was continuously on). The illumination on the sample is on for 1 s, then off for 1 s, with a 30 ms delay between the on/off states. Spectra with the light on and off were recorded in separate histograms. The relatively fast on/off modulation of the light minimized the temperature variations of the sample during the light on/off cycles. The temperature of the sample was monitored with a GaAlAs thermometer placed behind the sample. Positron and muon counters were arranged in standard configurations that were appropriate for LF-μSR and transverse field (TF)-μSR measurements (see Ref. 5 for more details).

III. PRECESSION SIGNATURES

This paper focuses on the influence of optical excitation on the precession signatures of Mu^+_{BC}, Mu^0_{BC}, and Mu^0_T. This section provides a reminder and/or overview of how these precession signatures can be obtained experimentally. All precession frequencies are intentionally chosen to reside in the window of 10–20 MHz.

The singly charged muonium center (such as Mu^+_{BC}) is studied in a transverse field of $\approx$0.1 T. Since no hyperfine interaction is associated with this center, the muon precesses at the Larmor frequency given by $\gamma_u H$, where the muon gyromagnetic ratio is γ_u=135.54 MHz/T and H is the magnitude of the applied field. An example of the spectra for Mu^+_{BC} is shown in Fig. 2(a). In the absence of illumination, there is very little relaxation of the muon polarization. Under illumination, a strong relaxation is observed [Fig. 2(b)].

The bond-centered muonium (Mu^0_{BC}) is studied in a longitudinal field of $\approx$0.2 T applied parallel to a $\langle 100 \rangle$ direction

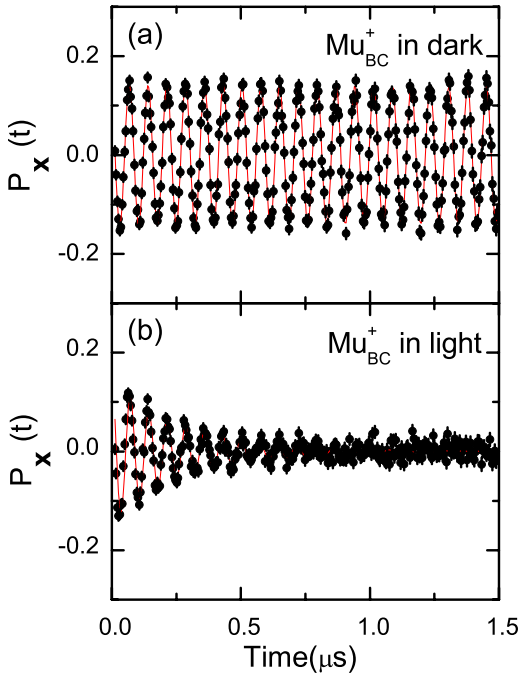

FIG. 2. (Color online) Typical TF-μSR spectra for Mu^+_{BC} in a field of 0.1 T and ≈260 K (a) in the dark and (b) under illumination. The circles are the experimental data and the solid lines are the fits as described in the text.

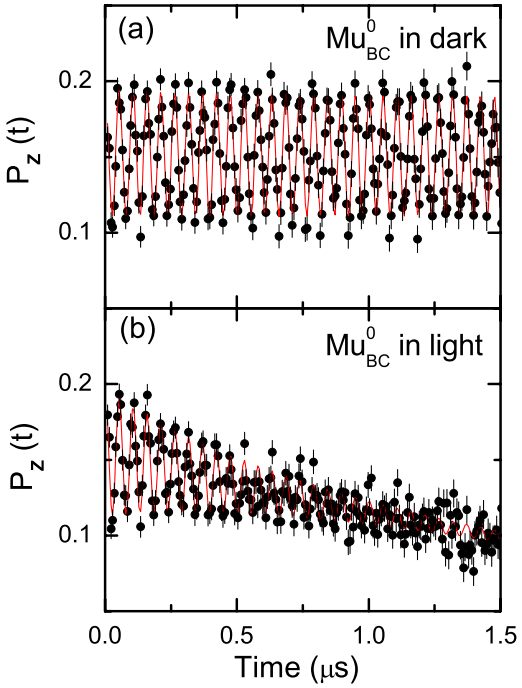

FIG. 3. (Color online) Typical LF-μSR spectra for Mu^0_{BC} in a field of ≈0.2 T and ≈64 K (a) in the dark and (b) under illumination. The circles are the experimental data and the solid lines are the fits as described in the text.

of the sample. At this magnetic field, about half of the muons can be thought of as precessing about an *effective* magnetic field that differs in both magnitude and direction from the applied field **H**. Hence, although the initial muon spin is parallel to **H**, a precessing signal of significant magnitude is observed. In addition, 0.2 T is close to a so-called "magic field," where the precession frequency (at ≈19.0 MHz) is essentially independent of the orientation between **H** and the Mu^0_{BC} hyperfine axis (also the bond axis).[15,35] Hence, in the absence of any dynamics, the muon spin polarization should be long lived. This is indeed the case, as seen in Fig. 3(a), for Mu^0_{BC} at low temperatures. However, under optical excitation, there are significant changes in the spectrum: In particular, as shown in Fig. 3(b), the precession signal shows significant relaxation with a noticeable $1/T_1$ component.

The muonium center Mu^0_T is characterized by an isotropic hyperfine parameter $A_\parallel = A_\perp \approx 2006$ MHz (at low temperatures) and is studied in a transverse field of $H \approx 1$ mT. Recall that at low fields, two of the precession frequencies, commonly referred to as ν_{12} and ν_{23} in the literature, are given to a very good approximation by $\gamma_e H/2$, where the electron gyromagnetic ratio $\gamma_e = 28\,025$ MHz/T. In our experiment, as indicated in Fig. 4(a), the precession frequency for this center occurs at ≈11.9 MHz. Note that there is significant relaxation of the unilluminated Mu^0_T signal at all temperatures. Above ≈75 K, illumination also produces relaxation of the Mu^0_T signal [see Fig. 4(b)].

The influence of optical excitation on the dynamics of the three muonium centers depends on the temperature of the sample and will be discussed in more detail in Sec. V. Nevertheless, it is qualitatively clear from Figs. 2–4 that there are dramatic differences in the muon polarization of all three centers in an illuminated sample compared to a sample in the dark. Hence, these results demonstrate that the precession signatures of the various muonium states in high resistivity Si can be dramatically affected by photoexcitation.

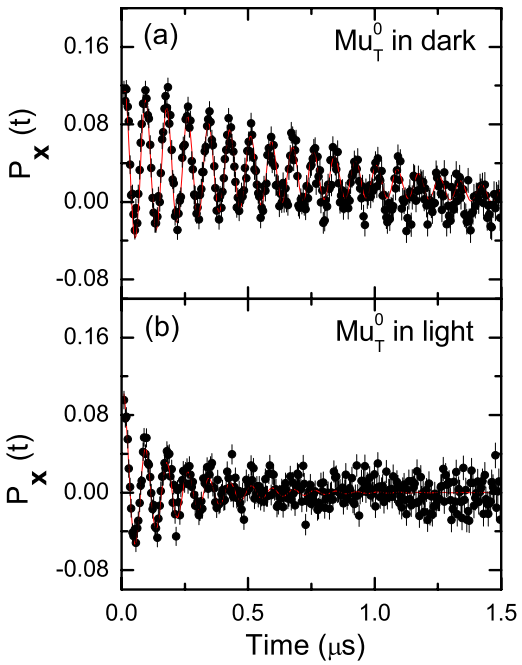

FIG. 4. (Color online) Typical TF-μSR spectra for Mu^0_T in a field of ≈1 mT and ≈269 K (a) in the dark and (b) under illumination. The circles are the experimental data and the solid lines are the fits as described in the text.

IV. DATA ANALYSIS

The quantities of interest that we extract from the precession data are the relaxation rates and the amplitudes associated with the three centers Mu_{BC}^{+}, Mu_{BC}^{0}, and Mu_{T}^{0}. The experimental precession data for Mu_{BC}^{+}, for which a typical spectrum is shown in Fig. 2, is well described by the function

$$P_x(t) = A_\mu e^{-\lambda_\mu t}\cos(\omega_\mu t + \theta_\mu), \tag{1}$$

where A_μ is the initial asymmetry, λ_μ is the relaxation rate, ω_μ is the muon Larmor precession frequency, and θ_μ is the phase of the signal.

The fitting function applied to the data associated with Mu_{BC}^{0}, such as that shown in Fig. 3, is

$$P_z(t) = A_{LF}e^{-\lambda_{LF}t} + A_{\mathrm{BC}}e^{-\lambda_{BC}t}\cos(\omega_{BC}t + \theta_{BC}). \tag{2}$$

The first term, characterized by initial asymmetry A_{LF} and exponential relaxation λ_{LF}, becomes noticeable upon optical excitation of the sample. As discussed in Sec. III, a precession signal due to Mu_{BC}^{0} is observed in a longitudinal field experiment close to the magic field. This is parametrized by the second term, which is characterized by the initial amplitude A_{BC}, the exponential relaxation parameter λ_{BC}, the Mu_{BC}^{0} precession frequency ω_{BC}, and the phase θ_{BC}.

The fitting function used to model the Mu_{T}^{0} data, such as that shown in Fig. 4, is

$$P_x(t) = A_T e^{-\lambda_T t}\cos(\omega_T t + \theta_T) + A_2 e^{-\lambda_2 t}\cos(\omega_2 t + \theta_2). \tag{3}$$

Since a precession signal due to Mu_{BC}^{+} can also be observed in the applied transverse field of 1 mT, the first term is used to describe Mu_{T}^{0} while the second term describes Mu_{BC}^{+}.

V. RESULTS AND DISCUSSION

The differences in the spectra observed under illumination and in the dark, such as those shown in Figs. 2–4, are attributed to interactions between muonium and the photogenerated carriers. The existence of these carriers enables processes that would otherwise be unimportant. In order to quantify the effects of optical excitation, we will examine the dynamics involved with the three muonium states Mu_{T}^{0}, Mu_{BC}^{0}, and Mu_{BC}^{+}. The Mu_{T}^{-} state is not included explicitly in our model since the maximum photoinduced carrier concentrations in this work remains below the threshold for a significant Mu_{T}^{-} formation. The functional forms, as well as the parameter values characterizing the transitions that are relevant for an *unilluminated* sample within this three-state model, has been discussed by Kreitzman *et al.*[8] and Hitti *et al.*,[28] i.e. in order to explain their rf-μSR (dark) Si data. In the analysis of our current data, we use the same functional forms for these transitions and also introduce additional processes that become important when the photoinduced carrier concentration becomes significant.

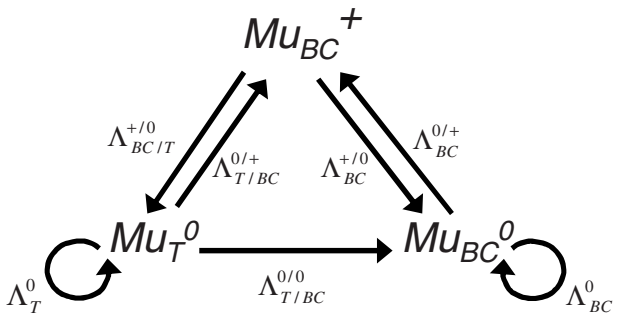

FIG. 5. The three-state model of muonium in Si under photoexcitation. The notation is described in more detail in the text.

This model is summarized in Fig. 5. As can be seen from Fig. 5, and as discussed in more detail below, we include the following dynamical interactions between Mu_{BC}^{+}, Mu_{BC}^{0}, and Mu_{T}^{0}: (i) Arrhenius thermally activated transitions, (ii) spin exchange processes involving Mu_{T}^{0} and Mu_{BC}^{0}, (iii) capture processes of electrons and/or holes, which lead to changes in the charge state, and (iv) "activated capture" processes which take the site change into account. The transition rate is denoted as Λ in the model, with the superscript representing the charge-state change and the subscript representing the site change. For example, a 0/+ superscript would indicate a transition of a neutral center to one that is positively charged, and a BC/T subscript would indicate that the muonium located at a BC site makes a transition to a T site. The symbols Λ_{T}^{0} and Λ_{BC}^{0} in Fig. 5 denote spin exchange processes involving Mu_{T}^{0} and Mu_{BC}^{0}, respectively.

The parameter values characterizing the dynamical interactions are summarized in Table I. They are inferred from simulations aimed at describing simultaneously the temperature dependences of the relaxation rates of all three muonium states. The simulated relaxation rates can be obtained by calculating the time evolution of the muon polarization within the dynamical model presented in Fig. 5; these are discussed in more detail in the Appendix.

Note that the initial amplitudes of the precession signatures of all three states are not affected by the optical excitation at any temperature, indicating that the photoexcitation does not change the implanted muon's initial state distribution significantly. [An example of this can be seen from the Mu_{BC}^{+} amplitude in Fig. 2 as well as in the inset of Fig. 6(b).]

We now discuss in more detail the relaxation rates associated with each of the three muonium centers Mu_{BC}^{0}, Mu_{BC}^{+}, and Mu_{T}^{0}. First, we address the Mu_{BC}^{0} center. As can be seen from Figs. 3 and 6(a), the Mu_{BC}^{0} precession signal shows little depolarization at low temperatures in the dark. However, there is an exponential increase in the dark relaxation rate beginning at $\approx$140 K, which by $\approx$170 K is too fast to be observed. This is attributed to the thermal ionization of Mu_{BC}^{0} into Mu_{BC}^{+} (i.e., $Mu_{BC}^{0} \rightarrow Mu_{BC}^{+} + e^{-}$).[4,8,26] An Arrhenius relation

$$\alpha_{BC}^{0/+}\exp^{(-E_{BC}^{0/+}/k_B T)}$$

($\alpha_{BC}^{0/+}$ is the prefactor frequency and $E_{BC}^{0/+}$ is the activation energy) can be used to characterize this ionization transition.

TABLE I. Transitions identified by the optical excitation experiment and their values.

Mu^0_{BC} relaxation		
Spin exchange	$\Lambda^0_{BC}=nv_n\sigma^0_{BC}$	$\sigma^0_{BC}=2(1)\times10^{-14}$ cm^2
Charge exchange		
$Mu^0_{BC}\rightarrow Mu^+_{BC}+e^-$	$\Lambda^{0/+}_{BC}=\alpha^{0/+}_{BC}\exp^{(-E^{0/+}_{BC}/k_BT)}+pv_p\sigma^{0/+}_{BC}$	$\alpha^{0/+}_{BC}=3.1(2)\times10^7$ MHz
$Mu^0_{BC}+h^+\rightarrow Mu^+_{BC}$		$E^{0/+}_{BC}=0.21(1)$ eV
		$\sigma^{0/+}_{BC}=4(1)\times10^{-15}$ cm^2
Mu^+_{BC} relaxation		
Charge exchange		
$Mu^+_{BC}+e^-\rightarrow Mu^0_{BC}$	$\Lambda^{+/0}_{BC}=nv_n\sigma^{+/0}_{BC}$	$\sigma^{+/0}_{BC}=3.3\times10^{-13}$ cm^2 (fixed)
$Mu^+_{BC}+e^-\rightarrow Mu^0_T$	$\Lambda^{+/0}_{BC/T}=nv_n\sigma^{+/0}_{BC/T}\exp^{(-E^{+/0}_{BC/T}/k_BT)}+$offset	$\sigma^{+/0}_{BC/T}=3(2)\times10^{-8}$ cm^2
		$E^{+/0}_{BC/T}=0.38(1)$ eV
		Offset=3 MHz
Mu^0_T relaxation		
Spin exchange	$\Lambda^0_T=nv_n\sigma^0_T$	$\sigma^0_T=2(2)\times10^{-15}$ cm^2
Site change		
$Mu^0_T\rightarrow Mu^0_{BC}$	$\Lambda^{0/0}_{T/BC}=\alpha^{0/0}_{T/BC}\exp^{(-E^{0/0}_{T/BC}/k_BT)}$	$\alpha^{0/0}_{T/BC}=2.5(5)\times10^7$ MHz
		$E^{0/0}_{T/BC}=0.38(1)$ eV
Charge exchange		
$Mu^0_T+h^+\rightarrow Mu^+_{BC}$	$\Lambda^{0/+}_{T/BC}=pv_p\sigma^{0/+}_{T/BC}\exp^{(-E^{0/+}_{T/BC}/k_BT)}$	$\sigma^{0/+}_{T/BC}=2.5(2)\times10^{-11}$ cm^2
		$E^{0/+}_{T/BC}=0.15(1)$ eV

The prefactor and the activation energy are found to be 3.1×10^7 MHz and 0.21 eV, respectively; both are in agreement with values obtained previously from rf-μSR experiments.[8,28] Note that the direct site-change transition $Mu^0_{BC}\rightarrow Mu^0_T$ is deemed unlikely due to the large energy barrier involved.[8] As a result, its contribution to the Mu^0_{BC} relaxation is omitted in the model (see Fig. 5). The optically induced relaxation rates of the Mu^0_{BC} signal at various temperatures are shown in Fig. 6(a). Clearly, the depolarization rate λ_{BC} under illumination is increased significantly compared to the dark for most temperatures. Two additional processes involving Mu^0_{BC} become important: spin exchange processes[11,26,29,30] with photogenerated electrons as well as capture processes with photogenerated holes ($Mu^0_{BC}+h^+\rightarrow Mu^+_{BC}$). These additional processes lead to depolarization of the Mu^0_{BC} signal even at low temperatures where thermal ionization of Mu^0_{BC} is not important. The spin exchange rate is set equal to $\Lambda^0_{BC}=nv_n\sigma^0_{BC}$, where n is the net electron density (estimated to be 8×10^{12} cm^{-3} under 100 W excitation[38]), v_n is the electron thermal velocity,[39] and σ^0_{BC} is the scattering cross section. Similarly, the hole capture rate is set equal to $pv_p\sigma^{0/+}_{BC}$, where p is the hole carrier density (set equal to n), v_p is the thermal velocity of holes, and $\sigma^{0/+}_{BC}$ is the hole capture cross section. In the dark, below $\approx$125 K, the relaxation associated with Mu^0_{BC} is small since the intrinsic concentrations of free carriers are small. The effects of spin exchange and hole capture processes are negligible here. However, under illumination, the free carrier concentrations increase dramatically and the relaxation rate is effectively increased by the amount $nv_n\sigma^0_{BC}+pv_p\sigma^{0/+}_{BC}$, with cross sections found to be $\sigma^0_{BC}=2\times10^{-14}$ cm^2 and $\sigma^{0/+}_{BC}$

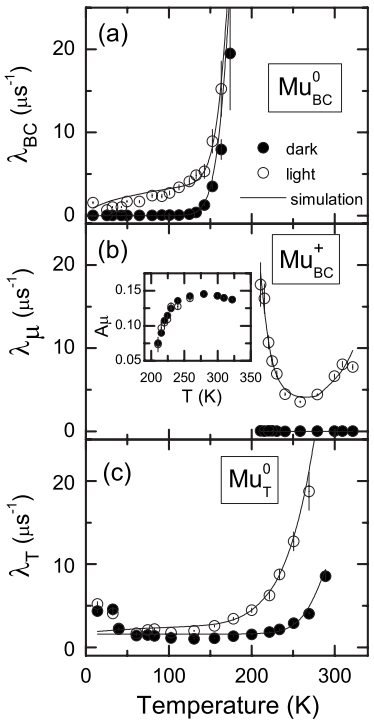

FIG. 6. Relaxation rates of the precession signals of (a) Mu^0_{BC}, (b) Mu^+_{BC}, and (c) Mu^0_T. The open and solid circles are data in the dark and under illumination, respectively. The solid lines are the simulations using the three-state model and the parameters listed in Table. I. (The power of the lamp is 200, 100, and 80 W for Mu^0_T, Mu^0_{BC}, and Mu^+_{BC}, respectively.) The inset in (b) shows the amplitude of the Mu^+_{BC} signal as a function of temperature.

$=4\times10^{-15}$ cm^2. These cross sections are assumed to be independent of temperature. Our value of the hole capture cross section $\sigma_{BC}^{0/+}$ is in reasonable agreement with the ones derived in Refs. 8 and 28. (It is notable that there is a slight temperature dependence of the Mu_{BC}^0 relaxation rates below $\approx$125 K, which may be dominated by the temperature dependence, i.e., $T^{1/2}$, of the carriers' velocities.)

Now, we turn to a discussion of the charged center Mu_{BC}^+. Consistent with previous measurements,[4] there is very little amplitude in the Mu_{BC}^+ precession signal below 200 K; hence, they are only investigated at temperatures higher than 200 K. (Recall that the majority of the implanted muons form either Mu_{BC}^0 or Mu_T^0 at low temperatures,[4] and the transition of these states into Mu_{BC}^+ must be "rapid enough" at high temperatures for a coherent precession signal to be observed.) In the dark, there is very little relaxation of the Mu_{BC}^+ signal. By contrast, significant relaxation is observed upon illumination, as indicated in Figs. 2 and 6(b). We propose, as indicated in Fig. 5, that the generation of photoelectrons and the subsequent electron capture by Mu_{BC}^+ make the following transition channels relevant: (i) $Mu_{BC}^+ + e^- \rightarrow Mu_{BC}^0$, and (ii) $Mu_{BC}^+ + e^- \rightarrow Mu_T^0$. The distinctive U-shaped temperature dependence for λ_μ, shown in Fig. 6(b), can be qualitatively understood as follows: In the region from $\approx$200 to 250 K, there exists a considerable ionization of the Mu_{BC}^0 to form Mu_{BC}^+, as evidenced by the significant precession amplitude of Mu_{BC}^+ [see inset of Fig. 6(b)]. This $\Lambda_{BC}^{0/+}$ conversion rate is significantly larger than the difference in precession frequencies associated with Mu_{BC}^+ and Mu_{BC}^0. At the same time, the existence of the photoelectrons now produces a significant rate for the reverse conversion from Mu_{BC}^+ to Mu_{BC}^0 due to electron capture. Hence, a cyclic charge exchange process develops ($Mu_{BC}^+ \leftrightarrow Mu_{BC}^0$). Since the transition rate $\Lambda_{BC}^{0/+}$ is very fast, we are in the "dynamically narrowed" regime: increasing the temperature and, hence, $\Lambda_{BC}^{0/+}$ leads to a *decrease* in the observed relaxation rate λ_μ. Above $\approx$250 K, another process becomes important in determining λ_μ: the conversion of Mu_T^0 into Mu_{BC}^+ (see the discussion below for details on Mu_T^0). This is evidenced by the increase in the dark values of λ_T above $\approx$250 K, as shown in Fig. 6(c). Thus, another charge exchange cycle ($Mu_{BC}^+ \leftrightarrow Mu_T^0$) develops. However, at these temperatures, the conversion rate $\Lambda_{T/BC}^{0/+}$ from Mu_T^0 to Mu_{BC}^0 is still slower than the difference in precession frequencies between Mu_T^0 and Mu_{BC}^+. The system is thus in the "dynamically broadened" regime whereby increasing the temperature results in an *increase* in λ_μ.

In order to obtain quantitative estimates of the transition rates, as listed in Table I, the electron capture process for $Mu_{BC}^+ + e^- \rightarrow Mu_{BC}^0$ is modeled by the expression $\Lambda_{BC}^{+/0} = n v_n \sigma_{BC}^{+/0}$, with the cross section $\sigma_{BC}^{+/0}$ fixed to the previously measured value of 3.3×10^{-13} cm^2.[28] This value is roughly the correct order of magnitude expected for a Coulombic capture cross section between a positively charged particle Mu_{BC}^+ and a negatively charged electron. The process $Mu_{BC}^+ + e^- \rightarrow Mu_T^0$, which involves changes in both the charge state and site (BC$\rightarrow T$), is modeled using the approach adopted in Ref. 8. It is assumed this activated capture process takes the following form:

$$n v_n \sigma_{BC/T}^{+/0} \exp^{-(E_{BC/T}^{+/0}/k_B T)}.$$

The estimated values of the relevant parameters are $E_{BC/T}^{+/0} = 0.38$ eV and $\sigma_{BC/T}^{+/0} = 3\times10^{-8}$ cm^2. While our activation energy $E_{BC/T}^{+/0}$ agrees with the previously reported value,[8,28] our activated cross section in this process is 2 orders of magnitude larger than the literature. The reason for this discrepancy is not well understood. It is worth noting that a small offset, assumed to be independent of temperature, is needed to fully model the λ_μ curve under illumination. This offset may suggest an additional capture process involving another diamagnetic state, e.g., Mu_T^-, that is not explicitly taken into account in our model.

Finally, we discuss the fast diffusing neutral center Mu_T^0. Figure 6(c) shows the temperature dependence of the Mu_T^0 relaxation λ_T. In the dark at low temperatures, there is already a significant relaxation of the precession signal, which is contrary to the behavior of Mu_{BC}^0 and Mu_{BC}^+. The mechanism for such a "background" relaxation, which has been observed previously in unilluminated silicon, was suggested to be due to interactions of the mobile Mu_T^0 with impurities in the material.[4] As the temperature increases beyond 240 K, the relaxation rates in the dark increase exponentially. This ionization process for Mu_T^0 is now widely accepted to be a two step process:[4,8] The Mu_T^0 first makes a transition to Mu_{BC}^0, where it is then converted into Mu_{BC}^+. The $Mu_T^0 \rightarrow Mu_{BC}^0$ transition can be described as an Arrhenius process

$$\Lambda_{T/BC}^{0/0} = \alpha_{T/BC}^{0/0} \exp^{(-E_{T/BC}^{0/0}/k_B T)},$$

and the subsequent $Mu_{BC}^0 \rightarrow Mu_{BC}^+$ transition has already been discussed above. The prefactor and the activation energy in the site-change process are found to be 2.5×10^7 MHz and 0.38 eV, respectively; both are similar with values obtained previously from rf-μSR experiments.[8,28] Under illumination, we propose that two additional processes involving Mu_T^0 become relevant: (1) the spin exchange and (2) the activated capture of holes to form Mu_{BC}^+. The spin exchange transition, modeled by the rate $n v_n \sigma_T^0$, is the primary cause of the relaxation in the low temperature region up to $\approx$175 K. In contrast to Mu_{BC}^0, a simple Arrhenius relation is not sufficient to describe the high temperature relaxation when there is an abundance of photogenerated carriers available. Instead, there appears to be an activated capture process that starts becoming important at $\approx$175 K. This is likely due to the hole capture of Mu_T^0 into the Mu_{BC}^+ state. In analogy to the activated electron capture process discussed above for Mu_{BC}^+, we model this rate as

$$\Lambda_{T/BC}^{0/+} = p v_p \sigma_{T/BC}^{0/+} \exp^{(-E_{T/BC}^{0/+}/k_B T)}.$$

The values that best simulate the data are found to be $E_{T/BC}^{0/+} = 0.15$ eV and $\sigma_{T/BC}^{0/+} = 2.5\times10^{-11}$ cm^2. The existence of such an activated hole capture process has also been

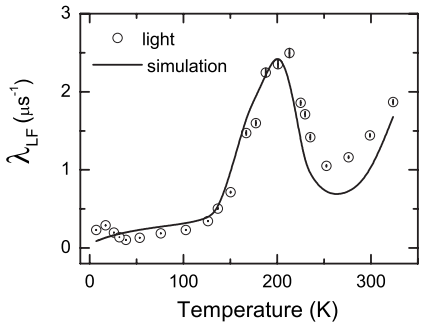

FIG. 7. Temperature dependence of the longitudinal field relaxation in an applied field of 0.1 T under illumination. The solid line represents the simulation using the model of Fig. 5 and the parameters in Table I.

suggested by a previous LF-μSR photoexcitation experiment.[29] However, no prefactor and activation energy parameters were deduced in this study.

The parameter values in Table I can also be used to simulate the temperature dependence of the longitudinal field relaxation λ_{LF}. The result is shown in Fig. 7 where the simulation is compared to the experimentally measured values of λ_{LF}: The agreement is reasonable. Qualitatively, the depolarization at low temperatures (less than 125 K) is dominated by the spin exchange of the neutral muonium states. The rapid rise at 140 K is predominantly due to the ionization (and recapture of photogenerated electrons) of the Mu^0_{BC}. The peak temperature at 200 K is where the Mu^+_{BC} enters the dynamically narrowed regime. Above 250 K, the site change $T \rightarrow$BC followed by the fast ionization becomes large enough to be observed.

Hence, our current results qualitatively support the general conclusions of previous photoexcitation experiments in silicon; i.e., muonium undergoes significant interactions with photogenerated electrons and holes. In addition, by making use of our ability to study the unique precession signatures associated with the three muonium states, the present work also provides more quantitative information on the parameters characterizing these photoinduced dynamics.

Finally, we note that previous LF-μSR photoexcitation studies on intermediate doped p-type and n-type Si (Ref. 29) as well as doped Ge (Ref. 37) have found evidence for a delayed formation of electrically inactive muonium. No clear evidence of such behavior is found in our current study of high resistivity Si. It may be interesting to apply our technique to investigate more heavily doped Si and Ge as well.

VI. CONCLUSION

In conclusion, we have demonstrated that optical excitation can dramatically enhance the relaxation of the precession signatures associated with Mu^+_{BC}, Mu^0_{BC}, and Mu^0_T in high resistivity silicon, hence providing detailed information on the dynamics, such as activation energies and capture cross sections, of the three major muonium states. A three-state model previously suggested to explain the radio-frequency data in unilluminated Si is a good description of the temperature dependence of the relaxation rates both in TF and LF modes, provided that the effects of photogenerated electrons and holes are taken into account in the spin exchange and carrier capture processes.

ACKNOWLEDGMENTS

This work is supported by the Natural Sciences and Engineering Research Council (NSERC), R.A. Welch Foundation, and the U.S. National Science Foundation. We would like to thank R. F. Kiefl, R. Kadono, and K. Shimomura for helpful discussions in the initial stages of this research.

APPENDIX: MODELING THE NET POLARIZATION

The calculation of the time-dependent muon polarization can be accomplished by using the formalism first described by Odermatt.[36] In short, the density matrix of a single muonium state, consisting of a muon and an electron, leads to a set of 15 coupled differential equations, which may be written compactly as

$$\frac{d\mathbf{P}}{dt} = \hat{M}\mathbf{P}. \tag{A1}$$

The polarization $\mathbf{P}$ is represented by a 15×1 vector that describes the state of the muon, its bound electron (in the case of neutral muonium), and the muon-electron interactions. In particular, the first three elements of $\mathbf{P}$ give the x, y, and z components of the muon polarization. The matrix $\hat{M}$ has a 15×15 dimension and is derived from the coupled differential equations; its matrix elements can be found in Ref. 36. The solution to Eq. (A1) is often expressed as

$$\mathbf{P} = \sum_{i=1}^{15} c_i \mathbf{a}_i e^{(-\alpha_i t)}, \tag{A2}$$

where the parameters $\mathbf{a}_i$ and α_i are the eigenvectors and (complex) eigenvalues of the matrix $\hat{M}$, respectively. The coefficient c_i is determined from the initial polarization at $t=0$. The effect of the spin exchange of neutral muonium is taken into account by subtracting $2\Lambda^0$ (the spin exchange rate) from the terms involving the bound electrons in the coefficient matrix $\hat{M}$.

In our model, there can be up to three muonium centers coexisting in the sample. Each of these centers can (in principle) make a transition to any of the other two centers. If the three centers are labeled as BC (Mu^0_{BC}), μ (Mu^+), and T (Mu^0_T), then Eq. (A1) is still formally correct, but with terms that should be interpreted as follows:[36]

$$\mathbf{P} = \begin{pmatrix} \mathbf{P}_{BC} \\ \mathbf{P}_{\mu} \\ \mathbf{P}_{T} \end{pmatrix} \tag{A3}$$

and

$$\hat{M} = \begin{pmatrix} \hat{M}_{BC} - (\Lambda_{BC}^{0/+} + \Lambda_{BC/T}^{0/0})I & \Lambda_{BC}^{+/0}A & \Lambda_{T/BC}^{0/0}A \\ \Lambda_{BC}^{0/+}A & \hat{M}_{\mu} - (\Lambda_{BC}^{+/0} + \Lambda_{BC/T}^{+/0})I & \Lambda_{T/BC}^{0/+}A \\ \Lambda_{BC/T}^{0/0}A & \Lambda_{BC/T}^{+/0}A & \hat{M}_{T} - (\Lambda_{T/BC}^{0/0} + \Lambda_{T/BC}^{0/+})I \end{pmatrix}. \tag{A4}$$

The term **P** is now a 45×1 vector that describes the polarizations of the three muon states simultaneously while the coefficient matrix $\hat{M}$ is a 45×45 matrix that contains the 15×15 matrices describing each isolated center (i.e., $\hat{M}_{BC}$, $\hat{M}_{\mu}$, $\hat{M}_{T}$). The notation for the transition rates in Eq. (A4) is the same as in Fig. 5. Rates located in the diagonal positions of Eq. (A4) are multiplied with a 15×15 identity matrix I. The off-diagonal elements are multiplied by a 15×15 matrix A. Matrix A is the same as the identity matrix if the electron polarizations are conserved during the transitions. However, if the electron polarizations are assumed to be lost during transitions, as in the case of thermal ionization of neutral centers into charged states, the diagonal elements of A involving electrons have to be zeroed ($A_{ii}=0$ for $i=4-15$).

*ifan@phys.ualberta.ca
†kimchow@phys.ualberta.ca

[1] S. M. Myers, M. I. Baskes, H. K. Birnbaum, J. W. Corbett, G. G. DeLeo, S. K. Estreicher, E. E. Haller, P. Jena, N. M. Johnson, R. Kirchheim, S. J. Pearton, and M. J. Stavola, Rev. Mod. Phys. **64**, 559 (1992).
[2] J. I. Pankove and N. M. Johnson, Semicond. Semimetals **34**, 1 (1991).
[3] C. G. Van de Walle and J. Neugebauer, Nature (London) **423**, 626 (2003).
[4] B. D. Patterson, Rev. Mod. Phys. **60**, 69 (1988).
[5] K. H. Chow, B. Hitti, and R. F. Kiefl, Semicond. Semimetals **51A**, 137 (1998).
[6] H. Simmler, P. Eschle, H. Keller, W. Kundig, W. Odermatt, B. D. Patterson, I. M. Savic, J. W. Schneider, B. Staublepumpin, U. Straumann, and P. Truol, Nucl. Instrum. Methods Phys. Res. B **63**, 125 (1992).
[7] R. Kadono, A. Matsushita, K. Nagamine, K. Nishiyama, K. H. Chow, R. F. Kiefl, A. MacFarlane, D. Schumann, S. Fujii, and S. Tanigawa, Phys. Rev. B **50**, 1999 (1994).
[8] S. R. Kreitzman, B. Hitti, R. L. Lichti, T. L. Estle, and K. H. Chow, Phys. Rev. B **51**, 13117 (1995).
[9] K. H. Chow, R. F. Kiefl, W. A. MacFarlane, J. W. Schneider, D. W. Cooke, M. Leon, M. Paciotti, T. L. Estle, B. Hitti, R. L. Lichti, S. F. J. Cox, C. Schwab, E. A. Davis, A. Morrobel-Sosa, and L. Zavieh, Phys. Rev. B **51**, 14762 (1995).
[10] K. H. Chow, B. Hitti, R. F. Kiefl, S. R. Dunsiger, R. L. Lichti, and T. L. Estle, Phys. Rev. Lett. **76**, 3790 (1996).
[11] K. H. Chow, R. F. Kiefl, B. Hitti, T. L. Estle, and R. L. Lichti, Phys. Rev. Lett. **84**, 2251 (2000).
[12] K. H. Chow, Physica B **326**, 145 (2003).
[13] B. E. Schultz, K. H. Chow, B. Hitti, Z. Salman, S. R. Kreitzman, R. F. Kiefl, and R. L. Lichti, Phys. Rev. B **72**, 033201 (2005).
[14] B. E. Schultz, K. H. Chow, B. Hitti, R. F. Kiefl, R. L. Lichti, and S. F. J. Cox, Phys. Rev. Lett. **95**, 086404 (2005).
[15] K. H. Chow, B. Hitti, and J. S. Lord, Phys. Rev. B **73**, 113202 (2006).
[16] Z. Salman, T. J. Parolin, K. H. Chow, T. A. Keeler, R. I. Miller, D. Wang, and W. A. MacFarlane, Phys. Rev. B **73**, 174427 (2006).
[17] R. L. Lichti, S. F. J. Cox, K. H. Chow, E. A. Davis, T. L. Estle, B. Hitti, E. Mytilineou, and C. Schwab, Phys. Rev. B **60**, 1734 (1999).
[18] K. H. Chow, B. Hitti, R. F. Kiefl, R. L. Lichti, and T. L. Estle, Phys. Rev. Lett. **87**, 216403 (2001).
[19] S. F. J. Cox, J. Phys.: Condens. Matter **15**, R1727 (2003).
[20] K. Shimomura, R. Kadono, K. Ohishi, M. Mizuta, M. Saito, K. H. Chow, B. Hitti, and R. L. Lichti, Phys. Rev. Lett. **92**, 135505 (2004).
[21] R. L. Lichti, W. A. Nussbaum, and K. H. Chow, Phys. Rev. B **70**, 165204 (2004).
[22] R. L. Lichti, H. N. Bani-Salameh, B. R. Carroll, K. H. Chow, B. Hitti, and S. R. Kreitzman, Phys. Rev. B **76**, 045221 (2007).
[23] R. C. Vilao, H. V. Alberto, J. P. Duarte, J. M. Gil, A. Weidinger, N. Ayres de Campos, R. L. Lichti, K. H. Chow, and S. F. J. Cox, Phys. Rev. B **72**, 235203 (2005).
[24] R. F. Kiefl, M. Celio, T. L. Estle, S. R. Kreitzman, G. M. Luke, T. M. Riseman, and E. J. Ansaldo, Phys. Rev. Lett. **60**, 224 (1988).
[25] J. W. Schneider, K. Chow, R. F. Kiefl, S. R. Kreitzman, A. MacFarlane, R. C. DuVarney, T. L. Estle, R. L. Lichti, and C. Schwab, Phys. Rev. B **47**, 10193 (1993).
[26] K. H. Chow, R. L. Lichti, R. F. Kiefl, S. Dunsiger, T. L. Estle, B. Hitti, R. Kadono, W. A. MacFarlane, J. W. Schneider, D. Schumann, and M. Shelley, Phys. Rev. B **50**, 8918 (1994).
[27] K. H. Chow, R. F. Kiefl, J. W. Schneider, B. Hitti, T. L. Estle, R. L. Lichti, C. Schwab, R. C. DuVarney, S. R. Kreitzman, W. A. MacFarlane, and M. Senba, Phys. Rev. B **47**, 16004 (1993).
[28] B. Hitti, S. R. Kreitzman, T. L. Estle, E. S. Bates, M. R. Dawdy, T. L. Head, and R. L. Lichti, Phys. Rev. B **59**, 4918 (1999).
[29] R. Kadono, R. M. Macrae, and K. Nagamine, Phys. Rev. B **68**, 245204 (2003).
[30] R. Kadono, A. Matsushita, R. M. Macrae, K. Nishiyama, and K. Nagamine, Phys. Rev. Lett. **73**, 2724 (1994).
[31] M. Iwanowski, K. Maier, J. Major, Th. Pfiz, R. Scheuermann, L. Schimmele, A. Seeger, and M. Hampele, Hyperfine Interact. **86**, 681 (1994).

[32] R. Scheuermann, J. Major, A. Seeger, L. Schimmele, J. Schmidl, and D. Herlach, Physica B **289-290**, 534 (2000).

[33] G. D. Morris, W. A. MacFarlane, K. H. Chow, Z. Salman, D. J. Arseneau, S. Daviel, A. Hatakeyama, S. R. Kreitzman, C. D. P. Levy, R. Poutissou, R. H. Heffner, J. E. Elenewski, L. H. Greene, and R. H. Kiefl, Phys. Rev. Lett. **93**, 157601 (2004); Z. Salman, A. I. Mansour, K. H. Chow, M. Beaudoin, I. Fan, J. Jung, T. A. Keeler, R. F. Kiefl, C. D. P. Levy, R. C. Ma, G. D. Morris, T. J. Parolin, D. Wang, and W. A. MacFarlane, Phys. Rev. B **75**, 073405 (2007); T. J. Parolin, Z. Salman, J. Chakhalian, Q. Song, K. H. Chow, M. D. Hossain, T. A. Keeler, R. F. Kiefl, S. R. Kreitzman, C. D. P. Levy, R. I. Miller, G. D. Morris, M. R. Pearson, H. Saadaoui, D. Wang, and W. A. MacFarlane, Phys. Rev. Lett. **98**, 047601 (2007); Z. Salman, D. Wang, K. H. Chow, M. D. Hossain, S. Kreitzman, T. A. Keeler, C. D. P. Levy, W. A. MacFarlane, R. I. Miller, G. D. Morris, T. J. Parolin, H. Saadaoui, M. Smadella, and R. F. Kiefl, *ibid.* **98**, 167001 (2007); Z. Salman, K. H. Chow, R. I. Miller, A. Morello, T. J. Parolin, M. D. Hossain, T. A. Keeler, C. D. P. Levy, W. A. MacFarlane, G. D. Morris, H. Saadaoui, D. Wang, R. Sessoli, G. G. Condorelli, and R. F. Kiefl, Nano Lett. **7**, 1551 (2007); M. Xu, M. D. Hossain, H. Saadaoui, T. J. Parolin, K. H. Chow, T. A. Keeler, R. F. Kiefl, G. D. Moris, Z. Salman, Q. Song, D. Wang, and W. A. MacFarlane, J. Mater. Res. (to be published).

[34] Z. Salman, E. P. Reynard, W. A. MacFarlane, K. H. Chow, J. Chakhalian, S. R. Kreitzman, S. Daviel, C. D. P. Levy, R. Poutissou, and R. F. Kiefl, Phys. Rev. B **70**, 104404 (2004); Z. Salman, R. F. Kiefl, K. H. Chow, M. D. Hossain, T. A. Keeler, S. R. Kreitzman, C. D. P. Levy, R. I. Miller, T. J. Parolin, M. R. Pearson, H. Saadaoui, J. D. Schultz, M. Smadella, D. Wang, and W. A. MacFarlane, Phys. Rev. Lett. **96**, 147601 (2006).

[35] A. Hintermann, P. F. Meier, and B. D. Patterson, Am. J. Phys. **48**, 956 (1980).

[36] W. Odermatt, Helv. Phys. Acta **61**, 1087 (1988).

[37] R. Kadono, R. M. Macrae, K. Nishiyama, and K. Nagamine, Phys. Rev. B **55**, 4035 (1997).

[38] The carrier density n is a sum of the intrinsic carriers and extrinsic carriers. The extrinsic carriers are generated by the optical excitation and is significantly larger than the intrinsic carrier density. The extrinsic carrier density is estimated by fitting the product $n v_n \sigma_{BC}^{+/0}$ to the Mu_{BC}^{+} relaxation while fixing the cross section to 3.3×10^{-13} cm^{-2}. In addition, because the intensity of the optical excitation used in the experiments is different for each of the three muonium centers, a different scaling multiplier is applied to the carrier density during the simulations of different muonium centers.

[39] The thermal velocity of electrons (or holes) can be calculated using the equipartition theorem, which yields $v_e = \sqrt{3 k_B T / m^*}$, where m^* is the effective mass of carriers in silicon.